

The nature of the calculation of the pressure in molecular simulations of continuous models from volume perturbations

Enrique de Miguel^{a)}

Departamento de Física Aplicada, Facultad de Ciencias Experimentales, Universidad de Huelva, 21071 Huelva, Spain

George Jackson^{b)}

Department of Chemical Engineering, Imperial College London, South Kensington Campus, London SW7 2AZ, United Kingdom

(Received 7 June 2006; accepted 21 September 2006; published online 30 October 2006)

We consider some fundamental aspects of the calculation of the pressure from simulations by performing volume perturbations. The method, initially proposed for hard-core potentials by Eppenga and Frenkel [Mol. Phys. **52**, 1303 (1984)] and then extended to continuous potentials by Harismiadis *et al.* [J. Chem. Phys. **105**, 8469 (1996)], is based on the numerical estimate of the change in Helmholtz free energy associated with the perturbation which, in turn, can be expressed as an ensemble average of the corresponding Boltzmann factor. The approach can be easily generalized to the calculation of components of the pressure tensor and also to ensembles other than the canonical ensemble. The accuracy of the method is assessed by comparing simulation results obtained from the volume-perturbation route with those obtained from the usual virial expression for several prototype fluid models. Monte Carlo simulation data are reported for bulk fluids and for inhomogeneous systems containing a vapor-liquid interface. © 2006 American Institute of Physics. [DOI: 10.1063/1.2363381]

I. INTRODUCTION

The usual approach to the evaluation of the pressure P in a molecular simulation involves an ensemble average of the instantaneous or microscopic pressure \mathcal{P} .^{1,2} For a system of N particles in a volume V , the microscopic pressure can be appropriately defined as¹

$$\mathcal{P} = \frac{1}{V} \left(\frac{1}{3} \sum_i m_i \mathbf{v}_i \cdot \mathbf{v}_i + \frac{1}{3} \sum_i \mathbf{r}_i \cdot \mathbf{f}_i \right), \quad (1)$$

where m_i is the mass, \mathbf{r}_i is the position, \mathbf{v}_i is the velocity, and \mathbf{f}_i is the force acting on particle i . In the absence of external fields, the only contribution to the forces arises from the intermolecular interactions. The macroscopic pressure P is simply obtained as $P = \langle \mathcal{P} \rangle$, where the angular brackets indicate either a time or statistical average over the appropriate ensemble. In the case of a system with pairwise interactions, the pressure can be written explicitly in the usual virial form as

$$P = \langle \rho kT \rangle + \left\langle \frac{1}{3V} \sum_i \sum_{j < i} \mathbf{r}_{ij} \cdot \mathbf{f}_{ij} \right\rangle, \quad (2)$$

where $\rho = N/V$ is the number density, k is the Boltzmann constant, T is the temperature, \mathbf{r}_{ij} is the intermolecular vector between a molecular pair, and \mathbf{f}_{ij} is the corresponding intermolecular force. The first term on the right-hand side of Eq. (2) is the kinetic (ideal gas) contribution and the second term

represents the residual contribution arising from the interactions.

This mechanical route to the calculation of the pressure in a simulation is particularly well suited when molecular dynamics is the technique of choice, as the evaluation of the forces is required to determine the molecular trajectories. Equation (2) can also be used for computing the pressure in a Monte Carlo simulation, albeit at the cost of an explicit calculation of the forces; in this case the calculation of the forces is not required for sampling the configuration space of the system. Though for most simple intermolecular potential models the evaluation is certainly straightforward, this may not be the case for complex intermolecular interactions, for which the evaluation of the forces can be rather involved or time consuming.³

An alternative route to the calculation of the pressure may be devised by starting from the thermodynamic relation for the change in Helmholtz free energy F in terms of changes in temperature and volume, $dF = -SdT - PdV$, where S is the entropy. As was first shown by Eppenga and Frenkel⁴ for systems of hard platelets and then by Harismiadis *et al.*⁵ for systems with continuous potentials, this thermodynamic route can be used to provide a simple expression that relates the equilibrium pressure to an average involving the Boltzmann factor associated with a small volume perturbation ΔV . Perturbative approaches of this kind (which stem from the seminal work of Longuet-Higgins,⁶ Barker,^{7,8} Pople,^{9,10} and Zwanzig¹¹) are referred to as single-stage free energy difference^{12,13} or “virtual-parameter-variation”¹⁴ methods. A derivation of the key expression is simple and is presented in Sec. II; we show in the Appendix that the thermodynamic

^{a)}Electronic mail: demiguel@uhu.es

^{b)}Electronic mail: g.jackson@imperial.ac.uk

relation is fully compatible with the virial route, cf. Eq. (2). The method, originally set in the canonical ensemble, can also be extended to the calculation of the pressure in other constant-volume ensembles, such as the microcanonical or grand canonical ensembles. An extension to the calculation of the components of the pressure tensor is straightforward.^{14,15}

Here, we report a detailed investigation of the adequacy of the volume-perturbation method for the calculation of the pressure in model systems characterized by continuous intermolecular interactions. Simulation data are reported at representative thermodynamic conditions for Lennard-Jones (LJ) systems, including homogeneous and inhomogeneous (vapor-liquid) states. Results are also reported for more complex systems in which the molecules interact through the Gay-Berne (GB) potential model.¹⁶ The latter is widely used in simulation of thermotropic liquid crystals (see Ref. 17 for a recent review). Particular emphasis is placed on the effect that the size and sign of the relative volume change $\xi \equiv \Delta V/V$ may have on the estimated value of the pressure. In all cases, a comparison is made with the calculated values of the pressure from the standard virial route. The results of this investigation are presented in Sec. III. Our conclusions are given in Sec. IV.

II. CALCULATING THE PRESSURE FROM A VOLUME PERTURBATION

For a system at constant N , V , and T , the pressure can be defined as

$$P = - \left(\frac{\partial F}{\partial V} \right)_{N,T} = kT \left(\frac{\partial \ln Q_{NVT}}{\partial V} \right)_{N,T}, \quad (3)$$

where Q_{NVT} is the partition function which in the canonical ensemble is given by

$$\begin{aligned} Q_{NVT} &= \frac{1}{\Lambda^{3N} N!} \int d\mathbf{r}^N \exp[-\beta \mathcal{U}(\mathbf{r}^N)] \\ &= \frac{V^N}{\Lambda^{3N} N!} \int ds^N \exp[-\beta \mathcal{U}(s^N)]. \end{aligned} \quad (4)$$

In this expression Λ is the de Broglie wavelength, \mathcal{U} is the configurational energy of the system, $\beta = (kT)^{-1}$, and s^N is a set of coordinates scaled with the linear dimensions of the system. As a generalization of the earlier work of Eppenga and Frenkel⁴ on hard-core particles, Harismiadis *et al.*⁵ presented an alternative method for the calculation of the pressure based on Eq. (3). The method amounts to a numerical estimate of the change in Helmholtz free energy under an isothermal volume perturbation. Following Harismiadis *et al.*,⁵ we consider a volume perturbation from V to $V' = V + \Delta V$, with $\Delta V > 0$. The associated change in free energy $\Delta F = F(V + \Delta V) - F(V)$ can be expressed as¹¹

$$\Delta F = -kT \ln \left(\frac{Q'}{Q} \right). \quad (5)$$

The ratio of partition functions can be cast in the form⁵

$$\begin{aligned} \frac{Q'}{Q} &= \frac{\int ds^N V'^N \exp[-\beta \mathcal{U}(V')] }{\int ds^N V^N \exp[-\beta \mathcal{U}(V)]} \\ &= \frac{\int ds^N V^N [(V'/V)^N \exp(-\beta \Delta \mathcal{U}^t)] \exp[-\beta \mathcal{U}(V)]}{\int ds^N V^N \exp[-\beta \mathcal{U}(V)]} \\ &= \left\langle \left(1 + \frac{\Delta V}{V} \right)^N \exp(-\beta \Delta \mathcal{U}^t) \right\rangle, \end{aligned} \quad (6)$$

where $\Delta \mathcal{U}^t = \mathcal{U}(V + \Delta V) - \mathcal{U}(V)$ is the energy associated with the increase in volume, and the angular brackets denote a configurational average in the canonical ensemble over the unperturbed system of volume V . Approximating the first derivative in expression (3) with a forward, finite-difference scheme one obtains

$$\frac{\partial F}{\partial V} \approx \frac{F(V + \Delta V) - F(V)}{\Delta V}, \quad (7)$$

and using Eq. (6), this yields the following expression for the pressure:

$$\begin{aligned} \beta P^+ &= \frac{1}{\Delta V} \ln \left\langle \left(1 + \frac{\Delta V}{V} \right)^N \exp(-\beta \Delta \mathcal{U}^t) \right\rangle \\ &= \frac{1}{\xi V} \ln \langle (1 + \xi)^N \exp(-\beta \Delta \mathcal{U}^t) \rangle. \end{aligned} \quad (8)$$

Here, the relative change in volume is denoted by $\xi \equiv \Delta V/V$, and the superscript $+$ refers to an increasing-volume (expansion) perturbation, which corresponds to $\xi > 0$. By straightforward manipulation, one may use the above result to recover the virial expression of the pressure (see the Appendix). Expression (8) suggests that the pressure can be calculated by averaging the Boltzmann factor associated with a virtual expansion of the system from V to $V + \Delta V$. This is closely related to Widom's¹⁸ method for the calculation of the chemical potential from a perturbation resulting from the insertion of a virtual particle, or to the test-area method¹⁹ for the computation of the surface tension from perturbations in the interfacial area at constant volume.

In principle, one could equally well have used a backward, finite-difference scheme to approximate the first derivative of the free energy. In this case one can write

$$\frac{\partial F}{\partial V} \approx \frac{F(V) - F(V - |\Delta V|)}{|\Delta V|}, \quad (9)$$

which results in an expression for the pressure of the form

$$\begin{aligned} \beta P^- &= \frac{1}{-|\Delta V|} \ln \left\langle \left(1 - \frac{|\Delta V|}{V} \right)^N \exp(-\beta \Delta \mathcal{U}^t) \right\rangle \\ &= \frac{1}{-|\xi| V} \ln \langle (1 - |\xi|)^N \exp(-\beta \Delta \mathcal{U}^t) \rangle, \end{aligned} \quad (10)$$

where $\Delta \mathcal{U}^t = \mathcal{U}(V - |\Delta V|) - \mathcal{U}(V)$ is the change in configurational energy associated with a perturbation that decreases the volume of the system from V to $V - |\Delta V|$. For systems of particles interacting through continuous potentials, P^+ and P^- are expected to be equal to the value of the pressure as long as $\Delta V \rightarrow 0$. In practical implementations, small but finite values of ΔV have to be used, and the forward and backward

approaches will not yield exactly the same value. A generally more reliable estimate of a first derivative is provided by the central, finite-difference approximation as follows:

$$\frac{\partial F}{\partial V} \approx \frac{F(V + \Delta V) - F(V - |\Delta V|)}{2|\Delta V|}. \quad (11)$$

In this case the pressure can clearly be expressed in the form

$$P^{\text{CD}} = \frac{1}{2}(P^+ + P^-), \quad (12)$$

with P^+ and P^- given by Eqs. (8) and (10). This expression suggests that the pressure can be computed from a combination of the averages of the Boltzmann factors associated with two virtual volume perturbations: one in which the volume changes from V to $V + \Delta V$ and the other from V to $V - |\Delta V|$. Introducing the two expressions for (8) and (10) into Eq. (12) yields

$$\beta P^{\text{CD}} = \frac{1}{2|\xi|V} \ln \frac{\langle (1 + \xi)^N \exp(-\beta \Delta \mathcal{U}^+) \rangle}{\langle (1 - |\xi|)^N \exp(-\beta \Delta \mathcal{U}^-) \rangle}. \quad (13)$$

Some care has to be exercised when using Eq. (13), as it implicitly assumes that both expansion and compression perturbations are appropriate to gauge the value of the pressure. This is expected to be valid for systems with continuous intermolecular potentials, but as was first noted by Eppenga and Frenkel⁴ the expression for the expansive perturbation is certainly not correct in the case of hard-core interactions. As an example, Eq. (8) does not yield the pressure for a system of hard spheres: a virtual perturbation in which the volume of the system is expanded yields $\Delta \mathcal{U}^+ = 0$, and P^+ therefore simply records the ideal-gas contribution; it is straightforward to show that in this case, expression (8) yields $P^+ = \rho kT$ in the limit of small ΔV . Though an expansion of the volume [cf. relation (13)] is not a valid route for the calculation of the pressure in the case of systems of hard particles, the pressure can still be evaluated according to Eq. (10) by considering compressive perturbations in which the volume is decreased. This is precisely the approach devised by Eppenga and Frenkel⁴ for evaluating the pressure in systems of hard particles. In the following study, we restrict ourselves to the case of systems characterized by continuous interactions.

The calculation of the pressure from a volume-perturbation scheme is not limited to the canonical ensemble, but can be easily generalized to other constant-volume ensembles. In the grand canonical ensemble, for example, Eqs. (8), (10), and (13) are still valid even though the number of particles N would now fluctuate; similarly, β would represent the inverse of the instantaneous (fluctuating) temperature in the case of simulations performed in the microcanonical ensemble. Expressions (8), (10), and (13) also apply to the calculation of the pressure in multicomponent systems and can be used in the semigrand canonical ensemble.²⁰

III. CALCULATING THE COMPONENTS OF THE PRESSURE TENSOR AND THE SURFACE TENSION FROM A VOLUME PERTURBATION

In an inhomogeneous system the pressure is generally a tensor property. There are a number of ways of generalizing the microscopic definition of the pressure to inhomogeneous

systems.²¹⁻²⁵ A suitable definition for the average (macroscopic) value of the components of the pressure tensor $P_{\alpha\beta}$ is²⁵

$$P_{\alpha\beta} = \langle \rho kT \delta_{\alpha\beta} \rangle + \frac{1}{V} \left\langle \sum_i \sum_{j>i} r_{ij}^\alpha f_{ij}^\beta \right\rangle, \quad (14)$$

where r_{ij}^α is the α component of the intermolecular vector \mathbf{r}_{ij} , and f_{ij}^β is the β component of the intermolecular force \mathbf{f}_{ij} . An alternative scheme, which does not require an explicit calculation of the derivative of the intermolecular potential, can be devised based on the thermodynamic definition of these components. For example, the diagonal Cartesian components of the pressure tensor $P_{\alpha\alpha}$ ($\alpha = x, y, z$) can be defined as

$$P_{\alpha\alpha} = - \left(\frac{\partial F}{\partial V} \right)_{N,T,L_{\beta \neq \alpha}}. \quad (15)$$

This derivative can be evaluated during a molecular simulation by performing a virtual volume perturbation in which the box dimension L_α is changed to $L_\alpha + \Delta L_\alpha$ while keeping all other dimensions L_β ($\beta \neq \alpha$) fixed. For a virtual expansion ($\Delta V/V = \Delta L_\alpha/L_\alpha > 0$), it follows that

$$\beta P_{\alpha\alpha}^+ = \frac{1}{\Delta V} \ln \left\langle \left(1 + \frac{\Delta V}{V} \right)^N \exp(-\beta \Delta \mathcal{U}^+) \right\rangle, \quad (16)$$

where $\Delta \mathcal{U}^+$ is the associated change in configurational energy. The corresponding canonical ensemble average is carried out over the unperturbed system. For a virtual decrease in the volume, where the box dimension L_α is decreased to $L_\alpha - |\Delta L_\alpha|$, it follows that

$$\beta P_{\alpha\alpha}^- = \frac{1}{-|\Delta V|} \ln \left\langle \left(1 - \frac{|\Delta V|}{V} \right)^N \exp(-\beta \Delta \mathcal{U}^-) \right\rangle. \quad (17)$$

In the case of a system with a continuous intermolecular potential $P_{\alpha\alpha}^+$ and $P_{\alpha\alpha}^-$ are again expected to yield good approximations to the actual value of the components of the pressure tensor provided ΔV (ΔL) is sufficiently small. For finite values of ΔV , a central difference approximation is expected to provide a more accurate estimate. As we have shown in the case of a homogeneous system, this approximation amounts to $(P_{\alpha\alpha}^+ + P_{\alpha\alpha}^-)/2$. As explained earlier, this expression is not appropriate for systems of hard-core particles; in this case, the components of the pressure tensor can be estimated from Eq. (17) for an appropriate virtual compression of the volume (box dimension).

A stringent validation of the approach can be provided from a computation of the components of the pressure tensor and the surface tension in an inhomogeneous system formed from two fluid phases separated by an interface. For a planar interface lying in the x - y plane, the components of the pressure tensor depend on the distance z to the interface. Mechanical arguments²⁴ lead to the expression

$$\gamma = \int_{-\infty}^{+\infty} dz [P_N(z) - P_T(z)], \quad (18)$$

where $P_N(z) = P_{zz}(z)$ is the local value of the normal pressure and $P_T(z) = P_{xx}(z) = P_{yy}(z)$ is the local value of the tangential pressure. For a planar interface, $P_N(z)$ is constant and equal

to the equilibrium pressure P ; by contrast, $P_T(z)$ is equal to P far from the interface, but becomes large and negative in its neighborhood. The calculation of γ from Eq. (18) requires the computation of the local values of the components of the pressure tensor. These are normally obtained in the course of a simulation as profiles along the z direction. The calculation of $P_N(z)$ and $P_T(z)$ by volume perturbation should pose no particular difficulty; Eqs. (16) and (17) can be used with $\Delta\mathcal{U}(z)=\mathcal{U}'(z)-\mathcal{U}(z)$ corresponding to the energy associated with the perturbation at each point z . We should note that there is some ambiguity in the definition of the *local* components of the pressure tensor,²⁴ but γ is well defined through Eq. (18).

As an alternative, we considered the calculation of the *macroscopic* averages of the components of the pressure tensor. A proper thermodynamic definition of these components is given by

$$P_N = - \left(\frac{\partial F}{\partial V} \right)_{N,T,L_x,L_y} = - \frac{1}{A} \left(\frac{\partial F}{\partial L_z} \right)_{N,T,A}, \quad (19)$$

$$P_T = - \left(\frac{\partial F}{\partial V} \right)_{N,T,L_z} = - \frac{1}{L_z} \left(\frac{\partial F}{\partial A} \right)_{N,T,L_z}, \quad (20)$$

where $A=L_xL_y$ is the area of the interface. One can easily show that the surface tension is related to the macroscopic averages defined in (19) and (20) simply through

$$\gamma = L_z(P_N - P_T). \quad (21)$$

This follows from the thermodynamic relation for the change in Helmholtz free energy of an inhomogeneous system, $dF = -SdT - PdV + \gamma dA$. At constant T and V , this reduces to $dF = \gamma dA$, which represents the thermodynamic definition of the surface tension. For a system with a planar interface, $F = F(N, T, V) = F(N, T, L_z, A)$ and the change in free energy can thus be written as

$$dF = \left(\frac{\partial F}{\partial L_z} \right)_{N,T,A} dL_z + \left(\frac{\partial F}{\partial A} \right)_{N,T,L_z} dA \\ = -AP_N dL_z - L_z P_T dA = \gamma dA, \quad (22)$$

where we have used the definitions in (19) and (20). Recalling that the change is at constant volume, $dV = AdL_z + L_z dA = 0$. Expression (21) follows by substituting $dL_z = -(L_z/A)dA$ into Eq. (22). One should note that the macroscopic components of the pressure correspond to the volume averages of their local component counterparts, $P_{\alpha\beta} = (1/V) \int d\mathbf{r} P_{\alpha\beta}(\mathbf{r})$.

The normal component P_N can therefore be calculated by computing the variation in free energy due to a volume perturbation where the box dimension L_z is changed but the area A of the interface remains constant.¹⁵ Similarly, the tangential component P_T follows from the variation of the free energy due to a volume perturbation in which A is changed keeping L_z constant; in this case the transverse box dimensions L_x or L_y could be changed separately or together to change A . The normal and tangential components can, in principle, be calculated by performing expansion (increasing

volume, +) or compression (decreasing volume, -) perturbations according to Eqs. (16) and (17), respectively.

IV. RESULTS AND DISCUSSION

All the simulations are performed according to a standard Metropolis Monte Carlo (MC) algorithm within the canonical ensemble (NVT). The Markov chain of states is divided into M blocks and the ensemble average $\langle A \rangle$ of any arbitrary property A is computed from the arithmetic mean of the coarse-grained (or block) averages \bar{A}_k , $k=1, \dots, M$. An estimate of the statistical precision of the sample average is given by the standard deviation in $\langle A \rangle$ calculated from $\bar{\sigma}/\sqrt{M}$, where $\bar{\sigma}$ is the variance of the block averages.²⁶ All thermodynamic quantities are expressed in conventional reduced units using the standard length (σ) and energy (ϵ) scales of the LJ and GB interactions. We use the usual convention $\rho^* = (N/V)\sigma^3$, $P^* = P\sigma^3/\epsilon$, $T^* = kT/\epsilon$, and $\gamma^* = \gamma\sigma^2/\epsilon$ to represent the reduced (dimensionless) number density, pressure, temperature, and surface tension, respectively.

A. Homogeneous systems

We first consider systems of $N=864$ LJ particles in cubic boxes of dimensions $L/\sigma=12, 10$, and 9 (number densities $\rho^*=0.5, 0.864$, and 1.185 , respectively) at a temperature of $T^*=1.5$, which correspond to supercritical fluid states. Two cases are analyzed: in the first instance, the interactions are spherically truncated and shifted (STS) at a cutoff distance r_c ; in the second, the interactions are simply spherically truncated (ST) at r_c . For the calculation of the pressure via the virial route, one needs to evaluate the forces. If $u(r)$ is the pair potential, the intermolecular force is given by $\mathbf{f} = f(r)\hat{\mathbf{r}}$, with $f(r) = -(du/dr)$ and $\hat{\mathbf{r}} = \mathbf{r}/r$.

For STS interactions, the potential is continuous at r_c where $f(r) = f_{\text{LJ}}(r)$ for $r < r_c$, and zero at distances beyond the cutoff. Here, $f_{\text{LJ}}(r) = -du_{\text{LJ}}(r)/dr$, with $u_{\text{LJ}}(r)$ being the LJ pair potential. For the ST interactions, one has to consider the impulsive force f_{imp} due to the discontinuity of the potential at r_c .²⁷ In this case, the pair interactions can be written as $u(r) = u_{\text{LJ}}(r)[1 - H(r - r_c)]$, where $H(r)$ is the Heaviside step function; it then follows that

$$f(r) = f_{\text{LJ}}(r)[1 - H(r - r_c)] + u_c \delta(r - r_c), \quad (23)$$

where $u_c = u_{\text{LJ}}(r_c)$ is the value of the LJ potential energy at r_c . The last term on the right-hand side of Eq. (23) represents the impulsive (attractive) force, which is by no means negligible,²⁷ and can make a significant contribution to the pressure. This contribution is explicitly given by

$$P_{\text{imp}} = \frac{1}{3V} \left\langle \sum_i \sum_{j>i} \mathbf{r}_{ij} \cdot \mathbf{f}_{\text{imp}} \right\rangle = \frac{1}{3V} r_c u_c \lim_{\Delta r_c \rightarrow 0} \frac{\langle n(r_c^+) \rangle}{\Delta r_c}, \quad (24)$$

where we have used a discrete representation of the delta function. Here, $\langle n(r_c^+) \rangle$ is the average number of molecular pairs between r_c and $r_c + \Delta r_c$. The impulsive pressure P_{imp} can thus also be expressed in terms of the radial distribution functions at $r=r_c^+$ as

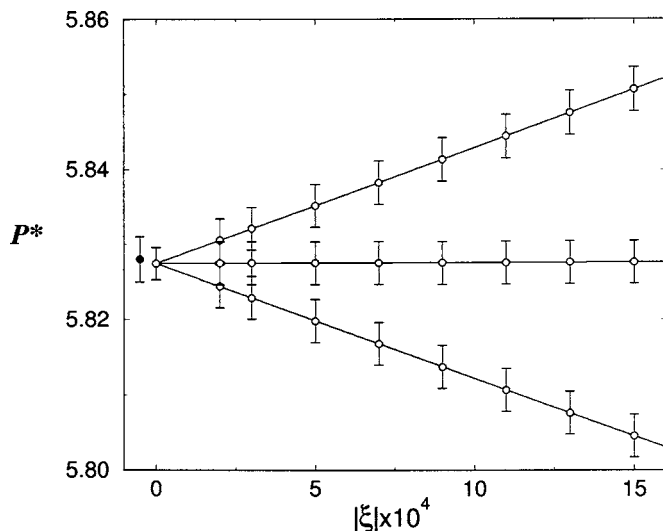


FIG. 1. The reduced pressure $P^* = P\sigma^3/\epsilon$ for a system of $N=864$ LJ particles with spherically truncated and shifted (STS) interactions (cutoff $r_c=2.5\sigma$) at a density of $\rho^* = \rho\sigma^3=0.864$ and temperature $T^* = kT/\epsilon=1.5$ as obtained from MC-NVT simulation using the volume-perturbation method for different values of the relative volume change $|\xi| = |\Delta V|/V$. The lines are linear fits through the data points. The lower curve corresponds to the results obtained from perturbations with $\xi > 0$ [forward difference Eq. (8)], the upper curve corresponds to the results obtained from perturbations with $\xi < 0$ [backward difference Eq. (10)], and the middle curve corresponds to the results obtained from a combined expansion/compression perturbation [central difference Eq. (13)]. The filled symbol represents the value of the pressure obtained from the virial route.

$$P_{\text{imp}} = \frac{2\pi}{3} \rho^2 g(r_c^+) u_c r_c^3. \quad (25)$$

This contribution is expected to be vanishingly small for large values of r_c , but one still has to proceed with caution. Ignoring the impulsive force does not affect the actual Markov chain in a MC simulation, but the calculated pressure is prone to systematic errors. The pressure determined here using the virial route for systems of particles interacting through the ST LJ potential explicitly incorporates the impulsive contribution. This is calculated from Eq. (24) by computing $\langle n(r_c^+) \rangle$ in a shell of radius r_c and width Δr_c . In most cases, a value $\Delta r_c = 0.005\sigma$ is used. One should note that in the calculation of the pressure through volume perturbations, no particular care has to be taken with the truncated attractive forces, as the method only involves the calculation of the configurational energy (and not the force).

In Fig. 1 we present the simulation data for the pressure of a STS LJ system with $r_c=2.5\sigma$ at $\rho^*=0.864$ and $T^*=1.5$ as obtained from Eqs. (8), (10), and (13) for relative volume changes $|\xi| \equiv \Delta V/V$ in the range $2 \times 10^{-4} \leq |\xi| \leq 15 \times 10^{-4}$. Once the system is equilibrated, averages are collected over 2×10^5 cycles, where one cycle amounts to N trial displacements of the molecules; the simulations are divided into $M=40$ blocks in order to estimate the errors. Isotropic virtual volume perturbations of magnitude ξ are performed every five cycles by rescaling the box length L of the simulation cell and the position of the molecular centers of mass according to the transformation $L' = (1 + \xi)^{1/3}L$ and $\mathbf{r}' = (1 + \xi)^{1/3}\mathbf{r}$ (r_c remains unchanged under this transformation). It is clear from the figure that the pressure exhibits a definite linear

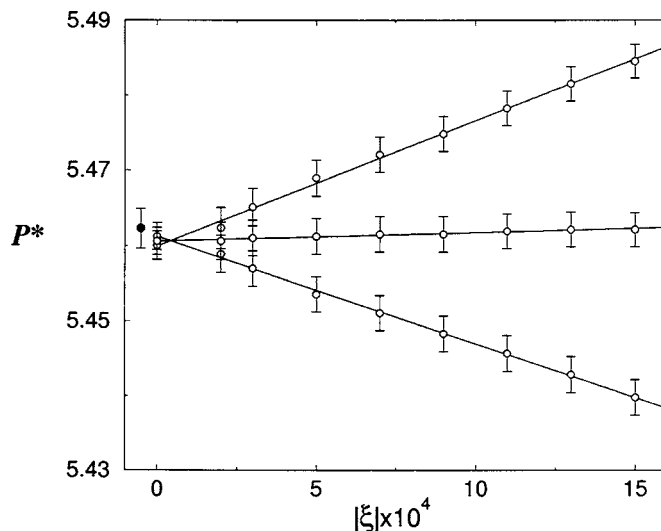


FIG. 2. Same as for Fig. 1, but for a system of $N=864$ LJ particles with spherically truncated (ST) interactions (cutoff $r_c=2.5\sigma$) at the same thermodynamic conditions. The filled symbol represents the value of the pressure obtained from the virial route with an explicit consideration of the impulsive contribution calculated according to Eq. (24).

behavior over the range of values of ξ considered here. The sets of data obtained from both expansive and compressive perturbations extrapolate cleanly to the same value $P^* = 5.827(2)$ when $|\xi| \rightarrow 0$. This value is consistent with the value of $P^* = 5.828(3)$ obtained from the virial route. An inspection of the figure indicates that as the size of the perturbation is made larger, the values of the pressure computed using the volume perturbation with a forward or backward difference scheme deviate systematically from the extrapolated value. For this thermodynamic state, the values of the pressure corresponding to the largest perturbation are $P^* = 5.805(3)$ and $5.851(3)$ for $\xi = 15 \times 10^{-4}$ and -15×10^{-4} , respectively, which are not within the estimated statistical errors of the extrapolated value of the pressure. By contrast, the values of the pressure obtained from a combined expansion-compression perturbation through the central difference scheme [cf. Eq. (13)] coincide fully with the extrapolated pressure. Moreover, these values appear to be rather insensitive to the size of the perturbation over the range of perturbations considered here (though this is, of course, expected to break down for large $|\xi|$). As one would expect, a finite central difference approximation to the first-order derivative is far superior to both the forward and backward difference approximations.

The results for the same thermodynamic state, but considering a LJ system with ST interactions at $r_c=2.5\sigma$, are shown in Fig. 2. In this case, the extrapolated values of the pressure are $(P^*)^+ = 5.461(2)$ and $(P^*)^- = 5.460(2)$, which are to be compared with the value $P^* = 5.462(3)$ resulting from the virial route. We should emphasize that these computations include the impulsive contribution. Neglecting this contribution yields an average value of the pressure of $P^* = 5.813(3)$. The approximate value of the impulsive contribution $P_{\text{imp}}^* \approx -0.40$ obtained from (25) with $g(r_c^+) \approx 1$ should be compared with the actual value $P_{\text{imp}}^* = -0.352(2)$ obtained from the simulation. The impulsive forces account for about

TABLE I. Values of the reduced pressure $P^* = P\sigma^3/\epsilon$ for Lennard-Jones (LJ) and Gay-Berne (GB) model systems as obtained by a linear extrapolation to $|\xi| \rightarrow 0$ of the values obtained from increasing-volume $(P^*)^+$ and decreasing-volume $(P^*)^-$ perturbations in MC-NVT simulations at different number densities $\rho^* = \rho\sigma^3$ and temperatures $T^* = kT/\epsilon$. Data in the last column correspond to the extrapolated values obtained from a combined compression-expansion perturbation $(P^*)^{\text{CD}} = [(P^*)^+ + (P^*)^-]/2$. $(P^*)^{\text{vir}}$ corresponds to the pressure obtained from the virial route. STS corresponds to spherically truncated and shifted interactions at a cutoff distance r_c ; ST corresponds to spherically truncated interactions.

Model	r_c/σ	$(P^*)^{\text{vir}}$	$(P^*)^+$	$(P^*)^-$	$(P^*)^{\text{CD}}$
$\rho^* = 0.50, T^* = 1.5$					
STS LJ	2.5	0.6764(9)	0.6765(7)	0.6765(7)	0.6765(7)
ST LJ	2.5	0.5475(9)	0.5472(7)	0.5472(7)	0.5472(7)
ST LJ ^a	2.5	0.6800(8)			
STS LJ	5.0	0.4479(7)	0.4476(6)	0.4476(6)	0.4476(6)
ST LJ	5.0	0.4317(9)	0.4315(7)	0.4315(7)	0.4315(7)
ST LJ ^a	5.0	0.4485(9)			
$\rho^* = 0.864, T^* = 1.25$					
STS LJ	2.5	5.828(3)	5.827(2)	5.827(2)	5.827(2)
ST LJ	2.5	5.462(3)	5.461(2)	5.460(2)	5.461(2)
ST LJ ^a	2.5	5.813(3)			
STS LJ	4.0	5.246(3)	5.246(2)	5.246(2)	5.246(2)
ST LJ	4.0	5.141(3)	5.141(2)	5.142(2)	5.141(2)
ST LJ ^a	4.0	5.241(3)			
$\rho^* = 1.185, T^* = 1.5$					
STS LJ	2.5	23.893(3)	23.893(3)	23.893(3)	23.893(3)
ST LJ	2.5	23.356(4)	23.347(2)	23.346(2)	23.347(2)
ST LJ ^a	2.5	23.810(4)			
STS LJ	4.0	22.779(4)	22.779(3)	22.779(3)	22.779(3)
ST LJ	4.0	22.675(4)	22.677(3)	22.677(3)	22.677(3)
ST LJ ^a	4.0	22.792(4)			
$\rho^* = 0.29, T^* = 1.25$					
STS GB	4.0	3.595(3)	3.595(2)	3.595(2)	3.595(2)
$\rho^* = 0.34, T^* = 1.25$					
STS GB	4.0	6.255(3)	6.255(2)	6.255(2)	6.255(2)

^aValue of the pressure neglecting the impulsive contribution.

6% of the contribution to the total pressure at these conditions. Simulation results for other thermodynamic conditions are collected in Table I.

The results included in Fig. 3 are obtained from a MC-NVT simulation of a crystalline (fcc) structure of $N=864$ molecules with a ST LJ potential truncated at $r_c=2.5\sigma$ confined in a cubic box of length $L=9\sigma$ ($\rho^*=1.185$). The NVT ensemble is not the most appropriate ensemble for the simulation of phases with translational order, but is intentionally chosen so as to validate the volume-perturbation method for the calculation of the components of the pressure tensor. The Cartesian components of the pressure tensor are computed with respect to a frame taken along the lengths of the simulation cell according to Eqs. (16) and (17). Any possible imbalanced stress resulting from the simulation setup should manifest itself in values of the components of the pressure tensor which are different from the bulk pressure. The resulting averages for the different components have been gathered in Table II. According to the results presented in Table II and Fig. 3, the components of the pressure tend to be slightly different from the bulk pressure at large values of $|\xi|$, both for expansion and compression volume perturbations (corresponding to the forward and backward difference schemes),

but they clearly converge to a common value, which coincides fully with the bulk pressure. As was found for the fluid state discussed earlier, the values of the pressure based on a central difference approximation are seen to be fairly insensitive to the magnitude of the perturbation. The values obtained from the virial route are slightly, but systematically, larger than those obtained from volume perturbations. This is related with the systematic error associated with the finite value of Δr_c used to evaluate the impulsive contribution. Full agreement between the virial and volume-perturbation routes would have been found if the impulsive contribution had been computed from an extrapolation of Eq. (24) to $\Delta r_c \rightarrow 0$. Once again, we stress that the impulsive contribution to the pressure is incorporated self-consistently into the volume-perturbation scheme.

We also test the performance of the volume-perturbation method for the calculation of the pressure in systems of non-spherical particles. The analysis is carried out for systems of Gay-Berne¹⁶ particles with cut and shifted (STS) interactions at $r_c=4\sigma$. The explicit form of the potential and the meaning of the parameters that define the model can be found elsewhere.¹⁶ Here we consider the original parameterization of the interaction model¹⁶ with model parameters $\kappa=3$

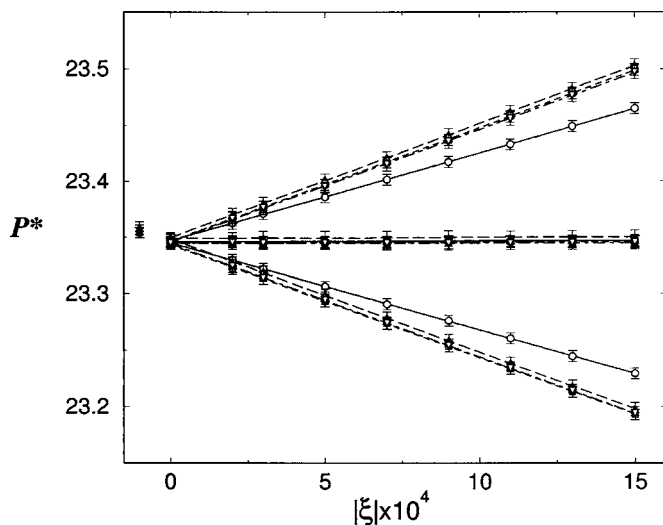


FIG. 3. Same as for Fig. 1, but for a system of $N=864$ LJ particles with spherically truncated (ST) interactions (cutoff $r_c=2.5\sigma$) in a fcc solid phase ($\rho^*=\rho\sigma^3=1.815$, $T^*=kT/\epsilon=1.5$). The data are represented for the bulk pressure (circles) $P^*=P\sigma^3/\epsilon$, the x component of the pressure tensor $P_{xx}^*=P_{xx}\sigma^3/\epsilon$ (squares), the y component of the pressure tensor $P_{yy}^*=P_{yy}\sigma^3/\epsilon$ (upward triangles), and the z component of the pressure tensor $P_{zz}^*=P_{zz}\sigma^3/\epsilon$ (downward triangles). The open symbols are the values obtained from the volume perturbations and the filled symbols are the corresponding values obtained from the virial route with an explicit consideration of the impulsive contribution calculated according to Eq. (24). The lines are linear fits through the data points.

(length-to-breadth ratio) and $\kappa'=5$ (energy anisotropy parameter). The phase diagram for this particular choice of parameters has been extensively studied by simulation.²⁸⁻³¹

We show in Fig. 4 the values of the pressure obtained from MC-NVT simulations of systems of $N=500$ GB particles at a reduced temperature of $T^*=1.25$ for number densities $\rho^*=0.29$ and 0.34 ; the data are included in Table I. According to previous work,³⁰ the low-density state corresponds to an orientationally disordered (isotropic) phase, while the high-density state exhibits orientational (nematic) order. The pressure of the isotropic-nematic transition at this temperature has been reported as $P^*=5.20$,³⁰ the corresponding densities at coexistence being $\rho_1^*=0.3152$ and $\rho_N^*=0.3219$. Volume perturbations are performed for values in the range $10^{-4} \leq |\xi| \leq 10 \times 10^{-4}$. All the conclusions drawn for the LJ systems apply to the GB systems, so clearly the molecular nonsphericity does not cause any particular problems.

TABLE II. Values of the Cartesian components of the pressure tensor (in units of ϵ/σ^3) for a crystalline (fcc) structure of 864 LJ molecules in a cubic box of length $L=9\sigma$ ($\rho^*=1.185$) at a reduced temperature of $T^*=1.5$ as obtained by a linear extrapolation to $|\xi| \rightarrow 0$ of the values obtained from increasing-volume (+) and decreasing-volume (-) perturbations in MC-NVT simulations. $P_{\alpha\alpha}^{\text{vir}}$ ($\alpha=x,y,z$) correspond to values obtained from the virial route. STS corresponds to spherically truncated and shifted interactions at a cutoff distance r_c ; ST corresponds to spherically truncated interactions.

Model	r_c/σ	P_{xx}^{vir}	P_{xx}^+	P_{xx}^-	P_{yy}^{vir}	P_{yy}^+	P_{yy}^-	P_{zz}^{vir}	P_{zz}^+	P_{zz}^-
STS LJ	2.5	23.895(4)	23.895(3)	23.895(3)	23.892(4)	23.893(3)	23.893(3)	23.891(5)	23.890(4)	23.890(4)
ST LJ	2.5	23.354(4)	23.343(4)	23.346(4)	23.358(6)	23.348(4)	23.350(4)	23.355(6)	23.344(4)	23.346(5)
ST LJ ^a	2.5	23.812(5)			23.808(4)			23.807(5)		
STS LJ	4.0	22.780(4)	22.779(3)	22.779(3)	22.779(3)	22.780(2)	22.780(3)	22.779(5)	22.778(4)	22.778(4)
ST LJ	4.0	22.682(4)	22.684(3)	22.684(3)	22.670(5)	22.672(4)	22.672(4)	22.677(4)	22.679(3)	22.679(3)
ST LJ ^a	4.0	22.794(5)			22.791(4)			22.791(4)		

^aValue of the components of the pressure tensor neglecting the impulsive contribution.

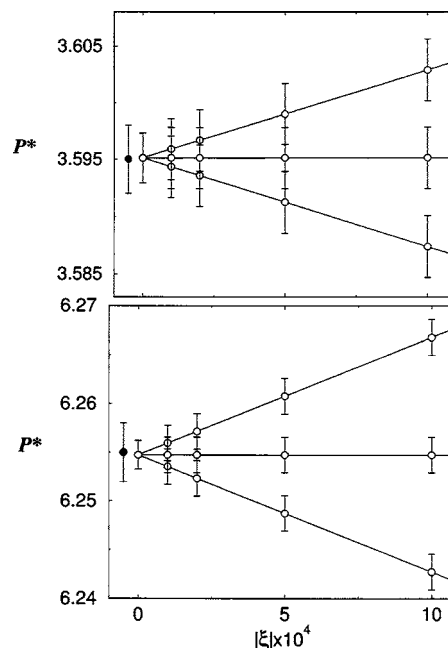


FIG. 4. The reduced pressure $P^*=P\sigma^3/\epsilon$ for a system of $N=500$ GB particles as obtained from volume perturbations in MC-NVT simulations with STS interactions at $r_c=4\sigma$. The isotropic phase at a reduced density $\rho^*=\rho\sigma^3=0.29$ and temperature $T^*=kT/\epsilon=1.25$ is shown in the upper panel; the nematic phase at $\rho^*=0.34$ and $T^*=1.25$ is shown in the lower panel. The meaning of the symbols is the same as in Fig. 1.

B. Inhomogeneous systems

In order to assess the applicability of the volume perturbation method for inhomogeneous systems, the macroscopic averages of the components of the pressure tensor P_N and P_T associated with the vapor-liquid interface of LJ and GB systems are calculated. A total of $N=1372$ particles are placed in a cubic box with sides of length $L=11.896\sigma$ for the LJ systems and $L=17.685\sigma$ for the GB systems. After an initial equilibration these liquid slabs are then placed in the middle of a simulation cell of dimensions $L_x=L_y=L$, $L_z=3L$ and the systems are allowed to equilibrate under constant NVT conditions. For a subcritical temperature and appropriate choice of density (box dimensions), this setup is expected to stabilize two planar vapor-liquid interfaces perpendicular to the z axis of the simulation cell. Once the systems are equilibrated, averages are collected over 2×10^6 MC cycles for the LJ systems and over 5×10^5 MC cycles for the GB systems.

TABLE III. MC-NVT simulation data for the macroscopic average normal $P_N^* = P_N \sigma^3 / \epsilon$ and tangential $P_T^* = P_T \sigma^3 / \epsilon$ components of the pressure tensor for the vapor-liquid interface in LJ and GB systems. Values of the surface tension $\gamma^* = \gamma \sigma^2 / \epsilon$ are determined according to Eq. (21). Estimated errors in the computed averages are reported as twice the standard error (i.e., 96% confidence level). The first column includes data obtained from the virial route; the second and third columns include data obtained from a linear extrapolation of the data to $|\xi| \rightarrow 0$ from increasing-volume ($\xi > 0$) and decreasing-volume ($\xi < 0$) perturbations, respectively. The fourth column are for data obtained from a combined compression/expansion perturbation. The last columns include MC or MD data from the literature. STS corresponds to spherically truncated and shifted interactions at a cutoff distance r_c ; ST corresponds to spherically truncated interactions.

	Virial	Forward	Backward	Central	MC	MD
STS LJ $T^* = 0.80$, $r_c = 2.5\sigma$						
P_N^*	0.0137(10)	0.0138(7)	0.0138(7)	0.0138(7)	0.0124 ^a	0.0140 ^a
P_T^*	-0.0092(10)	-0.0092(8)	-0.0092(8)	-0.0092(8)		
γ^*	0.409(5)	0.410(4)	0.410(4)	0.410(4)	0.405(3) ^a	0.408(18) ^a
ST LJ $T^* = 0.80$, $r_c = 2.5\sigma$						
P_N^*	0.0083(10)	0.0077(7)	0.0077(7)	0.0077(7)	0.0075 ^a	0.0080 ^a
P_T^*	-0.0252(12)	-0.0259(9)	-0.0259(9)	-0.0259(9)		
γ^*	0.598(7)	0.601(5)	0.600(5)	0.600(5)	0.618(9) ^a	0.623(28) ^a
ST LJ $T^* = 0.72$, $r_c = 2.5\sigma$						
P_N^*	0.0036(11)	0.0028(8)	0.0028(8)	0.0028(8)	0.0037 ^a	0.0028 ^a
P_T^*	-0.0389(1)	-0.0398(8)	-0.0398(8)	-0.0398(8)		
γ^*	0.759(6)	0.759(5)	0.760(5)	0.759(5)	0.743(3) ^a	0.748(12) ^a
STS GB $T^* = 0.59$, $r_c = 4.0\sigma$						
P_N^*	0.0010(7)	0.0010(6)	0.0010(6)	0.0010(6)		
P_T^*	-0.0122(11)	-0.0122(9)	-0.0122(9)	-0.0122(9)		
γ^*	0.348(16)	0.349(13)	0.349(13)	0.349(13)		0.37(7) ^b
STS GB $T^* = 0.67$, $r_c = 4.0\sigma$						
P_N^*	0.0021(7)	0.0024(6)	0.0024(6)	0.0024(6)		
P_T^*	-0.0052(8)	-0.0052(6)	-0.0052(6)	-0.0052(6)		
γ^*	0.195(7)	0.202(7)	0.202(7)	0.202(7)		0.18(5) ^b

^aReference 32.

^bReference 34.

Averages and estimates of the statistical uncertainties are computed by dividing the simulation into $M=20$ blocks. The macroscopic average of the normal component of the pressure P_N is computed from Eqs. (16) and (17) by averaging the Boltzmann factor associated with a volume perturbation in which the normal dimension of the simulation cell is changed from L_z to $L_z(1+\xi)$ while the transverse dimension remains unchanged. The macroscopic average of the tangential component P_T is calculated from (16) and (17) by considering a perturbation in which the tangential dimension of the system is changed isotropically from L_α to $L_\alpha(1+\xi)^{1/2}$, with $\alpha=x,y$, keeping L_z fixed. In both cases, $\xi = \Delta V/V$ defines the relative volume change associated with the perturbation. It is important to point out that this is different from the approach taken with the test-area method for the computation of the interfacial tension,¹⁹ where the changes in the normal and transverse dimensions are coupled to keep the overall volume constant. Both types of volume perturbations are performed every five cycles for a set of values of ξ , and in each case, the particle coordinates are rescaled according to the corresponding transformation.

Two temperatures, $T^* = 0.72$ and 0.80 , are considered for fluid systems with ST LJ interactions truncated at $r_c = 2.5\sigma$. For the higher temperature, an additional simulation is also carried out with STS interactions using the same value of the

cutoff. The corresponding results are collected in Table III. The reported values of the pressure obtained from the virial route in the case of ST interactions include the corresponding impulsive contributions calculated as before using a value $\Delta r_c = 0.005\sigma$ with Eq. (24). In line with our previous findings, the value of the pressure components obtained from the virial route is seen to differ slightly from the values computed from volume perturbations when considering ST interactions. As we have already mentioned for the homogeneous systems, this difference is due to the (small) systematic error resulting from the approximate procedure used here to evaluate the impulsive contribution in the virial relation. For systems with STS interactions, for which there are no such impulsive contributions, the data from both procedures are indistinguishable. A comparison with the data reported in the literature indicates consistency in the values of the normal and tangential components of the pressure and the corresponding interfacial tension.³²

The dependence of P_N , P_T , and γ on the size and sign of the volume perturbation is shown in Fig. 5 for the ST LJ system at $T^* = 0.72$. The data exhibit more scatter than those from simulations of homogeneous systems. In addition, the values obtained from the central difference approximation are seen to exhibit a larger degree of dependence with $|\xi|$ than in the case of homogeneous systems.

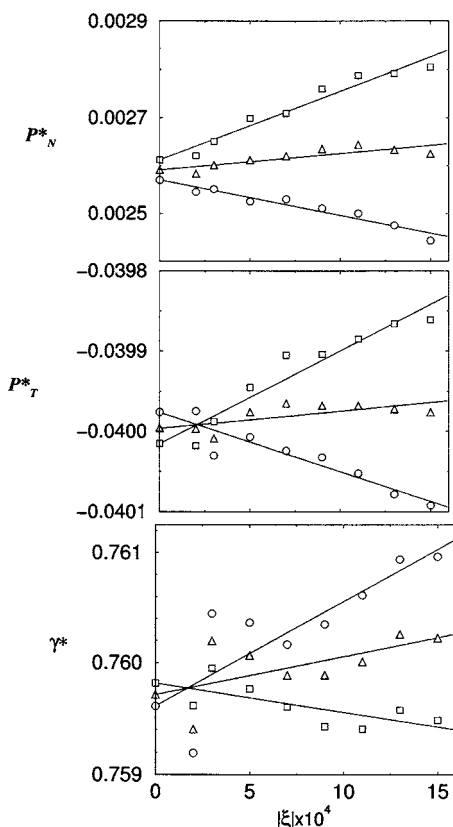


FIG. 5. The normal $P_N^* = P_N \sigma^3 / \epsilon$ and tangential $P_T^* = P_T \sigma^3 / \epsilon$ components of the pressure tensor and the surface tension $\gamma^* = \gamma \sigma^2 / \epsilon$ for the vapor-liquid interface in a system of LJ particles as obtained from volume perturbations in MC-NVT simulations with ST interactions at $r_c = 2.5\sigma$. The reduced temperature is $T^* = kT / \epsilon = 0.72$. Data are shown for different values of the relative volume change of the perturbation. The circles correspond to the results obtained from perturbations with $\xi > 0$ (forward difference scheme), the squares to the data for perturbations with $\xi < 0$ (backward difference scheme), and the triangles to the data from combined compression/expansion perturbations (central difference scheme). The absolute errors are larger than the vertical scale of the figures and are not shown for clarity.

Data from simulations of nonspherical GB molecules with STS interactions ($r_c = 4\sigma$) and model parameters $\kappa = 3$ (length-to-breadth ratio) and $\kappa' = 1$ (energy anisotropy parameter) are collected in Table III for temperatures of $T^* = 0.59$ and 0.67 . According to previous studies,^{33,34} the vapor-fluid critical temperature for this model is $T_c^* \approx 0.86$. The model exhibits a vapor-isotropic-nematic triple point at a temperature of $T^* \approx 0.63$. The fluid in coexistence with a vapor phase is thus expected to be orientationally disordered (isotropic) at $T^* = 0.67$ and orientationally ordered (nematic) at $T^* = 0.59$. Data obtained at the lower temperature are shown in Fig. 6. As with the other cases analyzed here, full agreement is found between the values obtained from the volume perturbation and virial routes.

We also calculate the surface tension using the test-area method,¹⁹ and the results are found to be indistinguishable from those obtained from the volume perturbations.

V. CONCLUSIONS

The nature of the volume-perturbation route to the calculation of the pressure in molecular systems characterized by continuous interactions is considered in this work. The

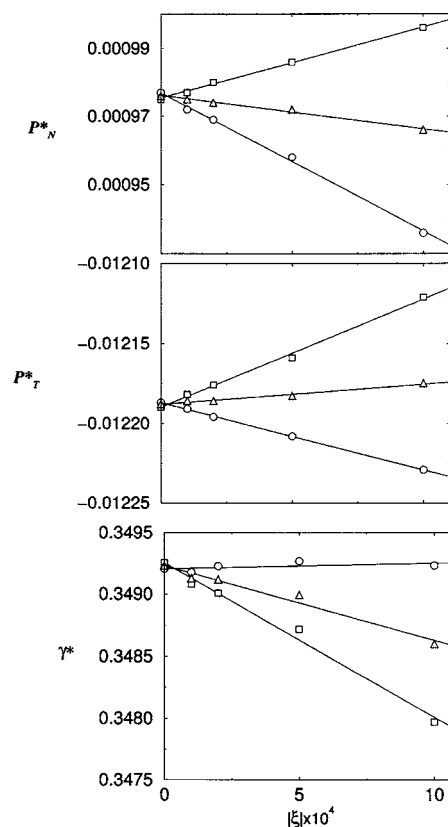


FIG. 6. The normal $P_N^* = P_N \sigma^3 / \epsilon$ and tangential $P_T^* = P_T \sigma^3 / \epsilon$ components of the pressure tensor and the surface tension $\gamma^* = \gamma \sigma^2 / \epsilon$ for the vapor-nematic interface in a system of GB particles with STS interactions ($r_c = 4\sigma$) as obtained from volume perturbations in MC-NVT simulations at a reduced temperature $T^* = kT / \epsilon = 0.59$. The meaning of the symbols is the same as in Fig. 5. The absolute errors are larger than the vertical scale of the figures and are not shown for clarity.

method amounts to estimating the change in the Helmholtz free energy associated with a test perturbation of magnitude $\xi = |\Delta V| / V$. In this approach one relates the pressure to a time or ensemble average of the Boltzmann factor associated with a change in the configurational energy for the perturbation. Both expansive and compressive perturbations are appropriate to gauge the value of the pressure as long as the magnitude of the perturbation is small enough or if the values are extrapolated to $|\xi| \rightarrow 0$. Though a degree of care is necessary in dealing with this type of extrapolation, a linear behavior is found for the range of value of $|\xi|$ and the thermodynamic conditions considered here. A combined compression-expansion perturbation to estimate the volume derivative of the free energy with a central finite-difference approximation provides accurate values of the pressure. This is due to the fact that finite-difference approaches which are based on central differences are typically (but not always) subject to smaller truncation errors than approximations based on forward or backward differences; central difference schemes are so-called second-order approaches, while forward or backward difference schemes are first-order approaches.

There must be some compromise when considering the optimal choice of $|\xi|$: the relative volume change should be small enough so that approximating a first-order derivative by a finite-difference scheme becomes justified, but not so small that the perturbation implies no appreciable changes in

the thermodynamic properties of the system. The combined compression-expansion approach not only yields accurate values of the pressure when compared with values obtained from the virial route, but also allows for larger volume perturbations (larger values of $|\xi|$) while keeping truncation errors to a minimum. It appears from the systems studied here that no extrapolation is required in practice when using a combined compression-expansion perturbation: a perturbation carried out for a single value of $|\xi|$ provides a reliable estimate of the pressure or the surface tension of inhomogeneous systems (at least as far as vapor-liquid coexistence is concerned).

We have shown that the volume perturbation and virial routes for calculating the pressure are fully consistent. As for the estimates of the errors in the computed averages, both methods appear to provide a similar level of accuracy, though smaller uncertainties are generally found when extrapolating the values obtained from volume perturbations to $|\xi| \rightarrow 0$. At first glance, the volume-perturbation method has an apparent advantage over the standard virial route in that no explicit evaluation of the forces is required. For simple intermolecular potential models this calculation is straightforward, and the volume-perturbation method does not therefore provide a real benefit. Arguably, the volume-perturbation method may be simpler to implement when the interactions are complex and the calculation of the forces becomes a complicated task; the algorithm can be programmed in a very efficient way to minimize the computational cost. In addition, the volume-perturbation method includes a natural way of treating contributions to the pressure arising from the discontinuities in the potential at the cutoff distance when the interactions are truncated. It is also fair to say that the corresponding impulsive contribution can be easily accounted for in simulations that make use of the virial route, though the precise implementation often requires some sort of extrapolation. An improper estimate of the impulsive contribution or, even worse, simply ignoring this contribution introduces a systematic error in the computed pressure. This can have a dramatic effect in the computed values of the pressure or the surface tension in fluid-fluid interfaces as has been pointed out by Trokhymchuk and Alexandre.³² From our experience, algorithms based on volume perturbations are also found to be slightly less demanding (in terms of computing time) than typical algorithms used in constant-pressure simulations. This not only applies to results obtained with volume-perturbation methods, but also to those obtained via the usual virial route. As far as precision is concerned, neither the volume perturbation nor the virial routes offer a significant advantage to constant pressure simulations at low pressures. This can be appreciated in the results for the vapor pressures that we report for the Lennard-Jones fluid: the relative errors are larger than they are at typical (higher pressure) thermodynamic conditions.

Systems of particles interacting through discontinuous potentials such as hard-core molecules or square-well systems pose additional challenges. In this case expansive and compressive perturbations are not generally expected to provide equivalent results for the pressure and interfacial tension (as can clearly be appreciated even for the simplest hard-

sphere system). An investigation of the nature of volume-perturbation methods in the calculation of the pressure from simulations of fluids characterized by hard interactions, including a comparison with the conventional virial route,³⁵ is currently under way and the results will be reported shortly.

ACKNOWLEDGMENTS

Financial support is due to the Spanish Dirección General de Investigación (Project No. FIS2004-06627-C02-01) and from Universidad de Huelva and Junta de Andalucía. Additional funding from the Engineering and Physical Sciences Research Council (EPSRC) of the UK (GR/N03358), (GR/N35991), and (GR/R09497), the Joint Research Equipment Initiative (JREI) (GR/M94427), and the Royal Society-Wolfson Foundation refurbishment scheme is gratefully acknowledged. Finally, we are both grateful to the Royal Society for the award of an International Short Visit grant which has facilitated our collaborative work.

APPENDIX: EQUIVALENCE OF THE THERMODYNAMIC AND VIRIAL EXPRESSIONS OF THE PRESSURE

For sufficiently small values of the size of the volume perturbation $\xi = \Delta V/V$, Eq. (8) can be expressed as

$$P = kT\rho + \frac{kT}{\xi V} \ln \langle \exp[-\beta \Delta \mathcal{U}(\xi)] \rangle, \quad (\text{A1})$$

where the dependence of the Boltzmann factor on ξ associated with the perturbation has been made explicit. Here, $\Delta \mathcal{U}(\xi) = \mathcal{U}'(\xi) - \mathcal{U}(0)$, with $\mathcal{U}'(\xi)$ and $\mathcal{U}(0)$ being the configurational energy of the perturbed and unperturbed systems, respectively. One can consider the coordinate transformation $x' = (1 + \xi)^{1/3}x$, $y' = (1 + \xi)^{1/3}y$, and $z' = (1 + \xi)^{1/3}z$, i.e., $\mathbf{r}' = (1 + \xi)^{1/3}\mathbf{r}$, and expand $\exp[-\beta \Delta \mathcal{U}(\xi)]$ in powers of ξ as follows:

$$\begin{aligned} \exp[-\beta \Delta \mathcal{U}(\xi)] &= \exp[-\beta \mathcal{U}'(\xi)] \exp[\beta \mathcal{U}(0)] \\ &= 1 - \beta \left(\frac{\partial \mathcal{U}'(\xi)}{\partial \xi} \right)_{\xi=0} \xi + \dots, \end{aligned} \quad (\text{A2})$$

where second-order terms have been neglected. One has

$$\begin{aligned} \frac{\partial \mathcal{U}'(\xi)}{\partial \xi} &= \sum_i \sum_{j>i} \frac{\partial u_{ij}(\mathbf{r}'_{ij})}{\partial \xi} \\ &= \sum_i \sum_{j>i} \frac{\partial u_{ij}(\mathbf{r}'_{ij})}{\partial \mathbf{r}'_{ij}} \cdot \frac{d\mathbf{r}'_{ij}}{d\xi} \\ &= -\frac{1}{3}(1 + \xi)^{-2/3} \sum_i \sum_{j>i} \mathbf{r}'_{ij} \cdot \mathbf{f}_{ij}(\mathbf{r}'_{ij}). \end{aligned} \quad (\text{A3})$$

Evaluating at $\xi=0$ yields

$$-\left(\frac{\partial \mathcal{U}'(\xi)}{\partial \xi} \right)_{\xi=0} = \frac{1}{3} \sum_i \sum_{j>i} \mathbf{r}_{ij} \cdot \mathbf{f}_{ij}(\mathbf{r}_{ij}). \quad (\text{A4})$$

Inserting (A4) into (A2) and substituting back into (A1) yields

$$P = kT\rho + \frac{kT}{\xi V} \ln \left\langle 1 + \frac{1}{3} \xi \sum_i \sum_{j>i} \mathbf{r}_{ij} \cdot \mathbf{f}_{ij} \right\rangle. \quad (\text{A5})$$

The virial expression of the pressure Eq. (2) is recovered using $\ln(1+x) \approx x$ in the limit of small x .

- ¹C. G. Gray and K. E. Gubbins, *Theory of Molecular Fluids: Fundamentals* (Oxford University Press, New York, 1984), Vol. 1.
²M. P. Allen and D. J. Tildesley, *Computer Simulation of Liquids* (Clarendon, Oxford, 1987).
³A. Cheng and K. M. Merz, *J. Phys. Chem.* **100**, 905 (1996).
⁴R. Eppenga and D. Frenkel, *Mol. Phys.* **52**, 1303 (1984).
⁵V. I. Harismiadis, J. Vorholz, and A. Z. Panagiotopoulos, *J. Chem. Phys.* **105**, 8469 (1996).
⁶H. C. Longuet-Higgins, *Proc. R. Soc. London, Ser. A* **205**, 247 (1951).
⁷J. A. Barker, *J. Chem. Phys.* **19**, 1430 (1951).
⁸J. A. Barker, *Proc. R. Soc. London, Ser. A* **219**, 367 (1953).
⁹J. A. Pople, *Proc. R. Soc. London, Ser. A* **215**, 67 (1952).
¹⁰J. A. Pople, *Proc. R. Soc. London, Ser. A* **221**, 498 (1954).
¹¹R. W. Zwanzig, *J. Chem. Phys.* **22**, 1420 (1954).
¹²D. A. Kofke and P. T. Cummings, *Mol. Phys.* **92**, 973 (1997).
¹³D. A. Kofke and P. T. Cummings, *Fluid Phase Equilib.* **150**, 41 (1998).
¹⁴H. L. Vörtler and W. R. Smith, *J. Chem. Phys.* **112**, 5168 (2000).
¹⁵J. K. Singh, D. A. Kofke, and J. R. Errington, *J. Chem. Phys.* **119**, 3405 (2003).
¹⁶J. G. Gay and B. J. Berne, *J. Chem. Phys.* **74**, 3316 (1981).

- ¹⁷C. M. Care and D. J. Cleaver, *Rep. Prog. Phys.* **68**, 2665 (2005).
¹⁸B. Widom, *J. Chem. Phys.* **39**, 2808 (1963).
¹⁹G. J. Gloor, G. Jackson, F. J. Blas, and E. de Miguel, *J. Chem. Phys.* **123**, 134703 (2005).
²⁰D. A. Kofke and E. D. Glandt, *Mol. Phys.* **64**, 1105 (1988).
²¹A. Harasima, *J. Phys. Soc. Jpn.* **8**, 343 (1953).
²²A. Harasima, *Adv. Chem. Phys.* **1**, 203 (1958).
²³S. Ono and S. Kondo, in *Handbuch der Physik*, edited by S. Flügge (Springer-Verlag, Berlin, 1960), Vol. 10, p. 134.
²⁴J. S. Rowlinson and B. Widom, *Molecular Theory of Capillarity* (Clarendon, Oxford, 1982).
²⁵P. Schofield and J. R. Henderson, *Proc. R. Soc. London, Ser. A* **379**, 231 (1982).
²⁶J. M. Haile, *Molecular Dynamics Simulation* (Wiley, New York, 1992).
²⁷D. Frenkel and B. Smit, *Understanding Molecular Simulation*, 2nd ed. (Academic, New York, 1996).
²⁸E. de Miguel, L. F. Rull, M. K. Chalam, K. E. Gubbins, and F. van Swol, *Mol. Phys.* **72**, 593 (1991).
²⁹E. de Miguel, L. F. Rull, M. K. Chalam, and K. E. Gubbins, *Mol. Phys.* **74**, 405 (1991).
³⁰E. de Miguel, *Mol. Phys.* **100**, 2449 (2002).
³¹E. de Miguel and C. Vega, *J. Chem. Phys.* **117**, 6313 (2002).
³²A. Trokhymchuk and J. Alejandre, *J. Chem. Phys.* **111**, 8510 (1999).
³³E. de Miguel, E. Martín del Río, J. T. Brown, and M. P. Allen, *J. Chem. Phys.* **105**, 4234 (1996).
³⁴E. Martín del Río and E. de Miguel, *Phys. Rev. E* **55**, 2916 (1997).
³⁵M. P. Allen, *J. Chem. Phys.* **124**, 214103 (2006).